Catena 226 (2023) 107066

Contents lists available at ScienceDirect

Catena

journal homepage: www.elsevier.com/locate/catena

Changes in soil hydrodynamic parameters during intermittent rainfall following tillage

F. Todisco [a], L. Vergni [a,*], M. Iovino [b], V. Bagarello [b]

[a] Department of Agricultural Food and Environmental Sciences, University of Perugia, Borgo XX Giugno, 74, 16121 Perugia, Italy
[b] Department of Agricultural, Food and Forest Sciences, University of Palermo, Italy, Viale delle Scienze, Buiding 4, 90128 Palermo, Italy

ARTICLE INFO

Keywords:
Soil porosity
Sorptivity
Hydraulic conductivity
Infiltration process
Soil sealing

ABSTRACT

The changes in the soil hydrodynamic properties following soil tillage were investigated in rainfall simulation trials of intermittent rain at the Masse experimental station (Soil Erosion LABoratory, SERLAB) in central Italy. The experiments were designed to build a database as representative as possible of situations that may occur in nature. The data collected during the experiments were used to determine the saturated soil hydraulic conductivity, K_s, the soil sorptivity at the antecedent soil–water matric potential Ψ_i, S, and the flow-weighted mean pore size at Ψ_i, λ_m. It was also verified if the energy content of total rainfall after tillage explained the short-term temporal variability of K_s. The results showed that during a sequence of rainfalls with wetting and drying cycles, there was a reduction of both S and K_s by 2.9–3.1 and 1.4–2.2 times, respectively, depending on the plot. This decrease was abrupt for S and more gradual for K_s. The analysis confirmed that K_s decreased as the overall energy dissipated at the soil surface, E, increased. The range of possible K_s values should be expected to become smaller as the dissipated rainfall energy after tillage increases ($\leq$30 mm/h for $E = 2$ kJ/m^2 and $\leq$ 5 mm/h for $E = 8$ kJ/m^2). For this reason, for the prediction and mathematical simulation of the rainfall-runoff transformation process, it is not advisable to limit the investigation to a single hydraulic characterization carried out immediately or shortly after tillage but data should be collected in a relatively long time span after tillage to properly characterize the soil in a condition favourable to surface runoff occurrence. For very high energy values, a recovery mechanism of the hydraulic properties of the altered/compacted layer was observed, but this behaviour should be confirmed by further investigations.

1. Introduction

Soil sorptivity, S, and saturated soil hydraulic conductivity, K_s, are the necessary soil parameters to describe infiltration in physically-based models of surface hydrological processes (e.g., Touma et al., 2007). Sorptivity defines the ability of a soil to conduct water by capillarity, and it varies with the initial and final soil water content and, when present, the depth of the water head at the soil surface. Saturated soil hydraulic conductivity represents the maximum water flow rate due solely to gravity in a completely saturated soil. The soil hydraulic conductivity expresses the aptitude of the porous medium to transmit water and, therefore, has a central importance in the surface runoff response and dynamics of hydrological processes. Generally, the hydraulic conductivity shows high space–time variability due to variations in both water content and soil physical properties (Mualem et al., 1990; Assouline and Mualem, 2006; Bagarello et al., 2019). Rainfall modifies these properties through wetting the soil and also because the energy of the impacting drops transferred to the porous medium partly compresses the surface soil layer and partly detaches soil particles and aggregates. The main changes of soil physical properties induced by the impacting rainfall are surface compaction, with an increase in bulk density (Mualem et al., 1990; Roth, 1997; Todisco et al., 2022) and the consequent decrease in the upper soil porosity and modification of soil micromorphology (Panini et al.; 1997; Rousseva et al, 2002); soil slaking caused by the compression of the air entrapped inside aggregates during wetting (Yoder, 1936; Le Bissonnais, 1996); aggregate breakdown by differential swelling (Kheyrabi and Monnier, 1968; Le Bissonnais, 1989); smoothening of the surface, with the material detached from the crest infilling the surface depressions (Zobeck and Onstad, 1987; Vinci et al., 2020); mechanical destruction of aggregates, that seals the pores and adds a further decrease in pore space and pore connectivity (Todisco et al., 2023). For this reason, raindrop impact is considered the main factor in

* Corresponding author.
E-mail addresses: francesca.todisco@unipg.it (F. Todisco), lorenzo.vergni@unipg.it (L. Vergni).

https://doi.org/10.1016/j.catena.2023.107066
Received 16 June 2022; Received in revised form 16 January 2023; Accepted 4 March 2023
Available online 12 March 2023

forming the soil crust, both depositional and structural (Farres, 1978; Bielders and Baveye, 1995). Ndiaye et al. (2005) showed that the time variation of the infiltration parameters (sorptivity and hydraulic conductivity) with cumulative rainfall/energy since tillage was due to the crust formation. Souza et al. (2014) clearly observed that a high mechanical resistance of soil, indicated by shear strength, was associated with the presence of soil crust. Furthermore, a highly significant negative correlation was found between soil shear resistance and both sorptivity and hydraulic conductivity. This negative correlation indicated that both S and K_s decreased significantly with the soil mechanical resistance increase and the presence of soil crust.

Decreasing roughness and sealing of soil pores, which occur as the first step toward crusting, decrease infiltration rates rapidly and pronouncedly, thus increasing runoff coefficients (Horton, 1939; Morin and Benyamini, 1977; Mualem et al., 1990; Assouline and Mualem, 1997; Schröder and Auerswald, 2000; Brakensiek and Rawls, 1983; Chu, 1985). Ben-Hur and Agassi (1997) found a significant correlation between the final infiltration rate and the soil erodibility values for different soils and rain intensities, suggesting that the same processes were responsible for both erosion and infiltration behaviour.

The temporal variability of hydraulic conductivity can be accentuated in tilled soils since tillage temporarily changes the structure of the surface soil layer where the infiltration processes take place (Coutadeur et al., 2002). An increase in K_s following tillage has been frequently observed (Haruna et al., 2018; Chahinian et al., 2006; Heard et al., 1988; Carter and Kunelius, 1986), and it can be generally attributed to an increase of both total porosity and macropores to micropores ratio. Ndiaye et al. (2005) found that the dynamics of the infiltration parameters (e.g., hydraulic conductivity) with cumulative rainfall/energy since tillage were explained by the crust types (Bielders et al., 1996) and their temporal dynamics of formation, both changing with tillage direction. However, in some circumstances, a reduction of K_s after tillage was also observed (Bhattacharyya et al. 2006; Joschko et al. 1992) as a consequence of the removal or decrease of the connectivity of the pore system present in the no-tilled soil. The increase of K_s after tillage is always temporary (Haruna et al., 2018) and is followed by a progressive reduction, whose dynamics is affected by soil type, agronomic practices, and environmental factors, primarily including rainfall.

The knowledge of the dynamics of K_s in tilled soils is expected to have a practical interest in the calibration and application of hydrological models, but this dynamics has not been analysed extensively in the literature. For example, Chahinian et al. (2006), studying the dynamics of different hydraulic properties in tilled silty-clay-loam soils, found that K_s decreased from a maximum value just after tillage to a minimum value after soil reconsolidation, at a rate dependent on the amount of rainfall that occurred since tillage. A similar dynamics was observed in a sandy-clay-loam soil by Ndaye et al. (2005), investigating the effect of intermittent rainfalls and tillage direction on the evolution of surface crusts, soil hydraulic properties and runoff generation. Remarkable variations of K_s over time were detected by Kargas et al. (2016) in both a cultivated and a non-cultivated bare soil, with minimum values prevailing during rainy periods and maximum values during dry periods. However, K_s varied only slightly in a non-cultivated soil covered by local weed vegetation.

The dynamics of other hydrological and physical properties affecting infiltration in tilled soils during an intermittent precipitation sequence has been less investigated. Vinci et al. (2020) studied the surface roughness dynamics in a dataset collected in experiments where three rainfall events followed initial tillage in a silty-clay-loam soil. Roughness decreased exponentially with cumulated rainfall and/or energy, and partial recovery was shown during the in-between-rains intervals. Todisco et al. (2022), analyzing the bulk density and infiltration dynamics of the same dataset, confirmed a quick and considerable decrease in porosity. Nevertheless, the decrease was not monotonic and continuous; on the contrary, it was counteracted by an increase during the desiccation period between successive rainfalls. The processes leading to the recovery of porosity were studied but prediction tools were not developed and appeared hard to be delineated, mainly due to the technical difficulties in measuring in great detail the dynamics of the single process. Evidently, control experiments examining a series of rainfall events in their effects on the hydrological processes of an evolving soil surface could contribute to partially fill this gap.

Rainfall simulation on small plots can be expected to yield a hydrologically plausible information on the dynamics of soil properties during intermittent rainfall since water is applied in a similar way to natural rainfall and the individual sampled area can be adapted, at least to some degree, for determining representative infiltration rate parameters for use in modelling field-scale flow processes. This experimental method is quite expensive and challenging, at least in the initial phases of design and realization of the equipment, and consequently most investigations on short term variability of soil hydraulic properties make use of water application procedures and sampling areas more practical but not directly referable to natural processes and relevant scales. The methodology by White et al. (1989) is potentially appropriate for the simultaneous determination of K_s, S and flow-weighted mean pore size at the antecedent potential Ψ_i, λ_m, from a rain simulation experiment. This methodology assumes that both the plot, having an area of nearly 1 m^2, and the surrounding area are wetted by rainfall. In some cases, this circumstance does not occur. For example, in the rainfall simulation experiments by Vinci et al. (2020) and Todisco et al. (2022), the plots are surrounded by an impermeable area (Vergni et al., 2018). The presence of the waterproof area implies that the surface directly wetted with the simulator is only that of the plot. If the soil is initially wet, this circumstance could be practically irrelevant. However, especially in initially dry soil conditions, it is not possible to exclude, during the test, the onset of lateral expansion phenomena of the wetting front due to capillarity. We could expect that lateral capillarity influences the infiltration process (e.g., Haverkamp et al., 1994), precluding the application of White's methodology. Therefore, in the case of experimental installations such as that described by Vergni et al. (2018), the irrelevance or the limited importance of lateral capillarity phenomena should be preliminarily ascertained in order to apply the White's methodology.

To sum up, i) too few hydrologically relevant data are currently available on short-term dynamics of soil hydrodynamic properties after tillage; ii) rainfall simulation at the small plot scale plus a simple data analysis method could help to reduce this gap with overall sustainable efforts; but iii) applying this methodology requires some preliminary check in particular experimental setting and circumstances due to a possible discordance between theory and practice.

The general objective of this paper is to examine the variation in the dynamics of the soil hydrodynamic properties during wetting and drying cycles following tillage. The specific objectives are to: 1) establish the relevance of lateral divergence processes induced by capillarity to analyze infiltration data; 2) determine the hydrodynamic properties of the soil during a period of intermittent rain; 3) verify if the energy of rainfall after tillage explains the short-term temporal variability of K_s.

2. Materials and methods

For the study, we used the hydrological data of several experiments conducted during the summer months of the 2016 to 2021 years, using the rainfall simulator available at the Masse experimental station (Vergni et al., 2018). The different types of experiments were designed accordingly to the purpose of the investigation. The simulator characteristics and the experiments are described in the following paragraphs.

2.1. Rainfall simulator characteristics

The rainfall simulator of the Masse experimental station (Fig. 1) is a nozzle-type rainfall simulator which operates simultaneously over two plots: plot 1 (P1) and plot 2 (P2) of 0.92 m^2 each (length 0.92 m, width 1 m and slope 16 %). The detailed technical features and rainfall

Fig. 1. The rainfall simulator of the Masse experimental station.

characteristics of the rainfall simulator can be found in Vergni et al. (2018); here, some relevant information is briefly summarized. The nozzles were centered over each plot at a mean height of 2.8 m above the ground. Two types of wide-angle square Full Jet nozzles, provided by Jetsystem srl (https://www.jetsystemsrl.it), were used in the experiments: the 14WSQ nozzle (intensity of about 40 mm/h and kinetic energy of 9.5 J/(mm·m^2)) and the 30WSQ nozzle (intensity of about 68 mm/h and kinetic energy of 14.5 J/(mm·m^2)). However, as detailed in the following paragraphs, we used the 14WSQ nozzle only for a few experiments in an initial wetting phase, IW, before the rainfall simulation, RS. The RSs were carried out using the 30WSQ nozzle in all the experiments.

Although the simulator was initially designed to produce rains of almost equal intensity in the two plots simultaneously, components wear progressively increased the differences in the intensity generated in the two plots (which are still<15%). Moreover, the environmental conditions (e.g., water temperature and network water pressure) could contribute to slight intensity variations among experiments and during experiments. For these reasons, we always made initial and final intensity checks for both plots in all experimental tests. The intensity checks were carried out by placing over the plots specifically designed covers that enable measuring the actual rain volume fallen in a fixed time interval, hence determining the actual rainfall intensity (Vergni et al., 2018).

2.2. Description of the experiments

The experiments consisted of a soil's manual harrowing to obtain a fine seedbed, almost 10 cm deep and with clods smaller than 5 cm, followed by one to four subsequent RSs with high-intensity rainfall ending when an almost steady-state runoff condition was reached. The experiments were classified according to three main types: in type-A experiment, the RS was conducted inserting a ring at the center of each plot to distinguish between the inner and the outer portion of the plot; in type-B experiment, the RSs sequence followed the tillage without a preliminary IW; in type-C experiment, the RS was preceded by an IW, which ended at ponding occurrence and increased the surface soil water content but did not generate runoff. Table 1 summarizes the main characteristics and data collected during these experiments. More details of each experiment type are given in the next paragraphs.

2.2.1. Type-A experiment

In this experiment, a ring was inserted within each plot, thus creating internal and external sub-plots whose areas are about 30% and 70% of the entire plot, respectively (Fig. 2). The experiment included two RSs (RS1 and RS2) of about 150 min, each preceded by an initial tillage and separated by an interval of 6 days. In the RS1, the external sub-plot of P2 was covered by a waterproof polyethylene sheet (Fig. 2) and the same was done for P1 in the RS2. Therefore, in P1 plot a RS over the entire area preceded a RS over the internal subplot. Conversely, in P2 plot a RS over the internal subplot preceded a RS over the entire plot. The runoff rate, r (mm/h), was measured at 5 min intervals sampling the total runoff; the rainfall intensity R (mm/h) was measured at the beginning and the end of each RS, placing specifically designed covers over the internal and the external sub-plots and following the same procedure described in section 2.1.

2.2.2. Type-B experiment

This experiment consisted of initial tillage followed by two or four RSs. The pause between two successive RSs varied from 4 to 7 days. Also, the RS duration was variable between 90 and 135 min. For each plot, the surface soil (upper 3.5 cm) water content, w (g/g), was measured by the gravimetric method before and after each RS. The soil bulk density, ρ_b (g/cm^3), was derived from the same samples. The rainfall intensity, R, was measured at the beginning and the end of each RS following the same procedure adopted in type A experiment; the runoff rate, r, was measured at 5 min intervals by sampling total runoff. The soil moisture content, θ (m^3/m^3), in the upper 15 cm at the beginning and the end of each RS was also measured by a portable Time Domain Reflectometry device. The time to ponding, t_{ps} (min), and the time to runoff, t_{ds} (min), were also visually determined.

Table 1
Characteristics and information considered for the different types of rainfall simulation experiments. IW: Initial Wetting; RS: Rainfall Simulation; R; rainfall rate; r: runoff rate; w: gravimetric water content; θ: volumetric water content; ρ_b: soil bulk density; t_{ps}: time to incipient ponding; t_{ds}: time to runoff. The database includes 14 RS for each plot.

Experiment type	IW before RS	Number of experiments	N° of RSs after tillage	R	r	w	θ	ρ_b	t_{ps}	t_{ds}
A	No	2	1	•	•					•
B	No	1	2	•	•	•	•	•	•	•
		1	4	•	•	•	•	•	•	•
C	Yes	2	3	•	•					•

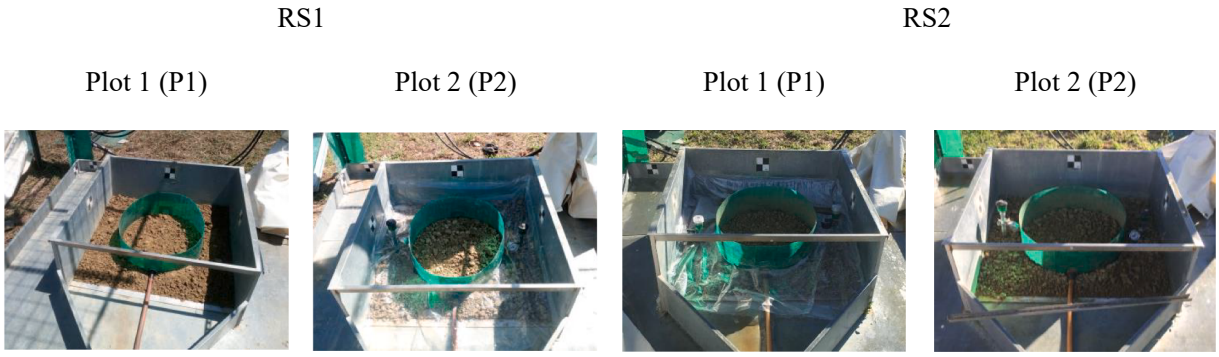

Fig. 2. Setup of type-A experiment including two RSs (RS1 and RS2), each preceded by initial tillage. During RS1, the external sub-plot of P2 was covered by a waterproof polyethylene sheet and the same was done for P1 during RS2. Conversely, a RS over the entire plot was carried out in P1 during the RS1 and in P2 during RS2.

2.2.3. Type-C experiment

Each type-C experiment consisted of initial tillage and three RSs following an IW. The three RSs were separated by a few days and started a few minutes after the IW (Table 1). This experiment was replicated two times on both P1 and P2, with a pause of a few months between the experiments. The IW duration was 30 min or more, while the RS duration varied between 60 and 120 min. The water content, w, bulk density, ρ_b, and rainfall intensity, R, before and after IW and RS, and the runoff rate, r, during each RS were measured following the same procedure adopted for type-A and type-B experiments.

2.2.4. Experimental design

The different types of experiments were designed for various purposes.

The type-A experiment aimed to check the usability of the methodology by White et al. (1989) for determining soil hydrodynamic properties at the Masse experimental station. This methodology referred to a spatially distributed process, and its use in this investigation was justified if it was possible to assume that the flow did not undergo a significant lateral divergence due to capillarity even if the wetted area was only that of the plot (Fig. 1). In type-A experiment, we can assume that, due to the plot's setup (Fig. 2), lateral divergence was prevented for the inner ring of the P1 plot but not for that of the P2 plot during RS1. Opposite conditions were instead designed for RS2, that was lateral divergence was possible for the inner ring of the P1 plot but not for that of the P2 plot.

The type-B and type-C experiments aimed to evaluate the temporal evolution of hydrodynamic variables and determine the relationship between the saturated hydraulic conductivity, K_s, and the cumulative rainfall kinetic energy, E, under different soil initial conditions. The distinction between type-B and type-C experiments was motivated by the intention to build a database as representative as possible of situations that may occur in nature: severe events from the beginning (type-B) and intense events preceded by a light rain (type-C). This implied a further difference between the two types of experiments, as the effect of a severe event on initially dry (type B) or wet (type C) soil was simulated.

2.3. Estimation of saturated soil hydraulic conductivity, sorptivity, and flow-weighted mean pore size

The data collected during rainfall simulation experiments were used to determine the saturated soil hydraulic conductivity, K_s (m/s), the soil sorptivity at the antecedent soil–water matric potential Ψ_i, S (m/ $s^{0.5}$), and the flow-weighted mean pore size at the antecedent potential Ψ_i, λ_m (m) (White et al. 1989). In particular, K_s was assumed to be equal to the infiltration rate, ir (m/s), at the nearly steady conditions reached at the end of each RS:

$$K_s = R - r \tag{1}$$

An estimate of S and λ_m was obtained by the following relationships:

$$S = \left[\frac{1.818R(R-r)t_{ps}}{ln\left(\frac{R}{r}\right)}\right]^{\frac{1}{2}} \tag{2}$$

$$\lambda_m = \frac{\Delta\theta K_s \sigma}{0.55\rho g S^2} \tag{3}$$

where, in addition to the variables already defined, $\Delta\theta$ (m^3/m^3) is the difference between the volumetric water content of the saturated soil (θ_s) and the antecedent volumetric soil water content (θ_i), σ and ρ are the surface tension and density of the soil water (7.28×10^{-2}N/m and 998.21 kg/m^3, respectively, for pure water at 20° C), and g is the acceleration due to gravity. An estimate of t_{ps} can be obtained by the visual appearance of water at the soil surface (White et al., 1989). The concentration of λ_m pores, N_0 (number of pores/m^2), can be estimated using Poiseuille's law for flow in a capillary tube as (Reynolds et al., 1995):

$$N_0 = \frac{8\mu K_s}{\rho g \pi \lambda_m^4} \tag{4}$$

where μ ($8.94 \cdot 10^{-4}$ kg / m s) is the dynamic viscosity of water. Eq.(4) provides an estimate of the number of λ_m pores per unit infiltration surface that are required to produce the measured K_s value (Reynolds et al., 1995; Iovino et al., 2016).

3. Results

3.1. Dimensional characteristics of the infiltration process during rainfall simulation

Equation (1) assumes the absence of any lateral divergence of the wetting front during the infiltration process. Therefore, the use of the methodology by White et al. (1989) in this investigation was justified if it was possible to recognize that flow did not undergo a significant lateral divergence due to capillarity. This hypothesis can be formulated because: i) the plots are relatively large (about 1 m^2); ii) the experiment consists of a succession of events; iii) in some cases, the RS was preceded by a pre-wetting stage. Moreover, it could also be presumed that the subsurface flow of the infiltrated water reduces the expansion of the wetting front at the lateral sides and the top of the plot. In this paragraph, the passage from the hypothesis formulation to its experimental check was carried out.

Fig. 3 shows the dynamics of rainfall rate, *R*, runoff, *r,* and infiltration, *ir*, observed during the two successive RS1 and RS2 in the internal rings of both P1 and P2.

With reference to the P1 plot (Fig. 3a), simulated rainfall rates for the RS1, wetting the entire plot area, and RS2, wetting only the inner ring area, were very similar. During the experiments, clear correspondences can be observed regarding the temporal behaviour of both runoff and infiltration rates. The time at which the *r* and *ir* values were equal was rather similar for the two RSs (nearly 0.67 h for RS1 and nearly 0.58 h for RS2). Finally, similarities were detected with reference to the final runoff rate (r = 59.1 and 60.5 mm/h for RS1 and RS2, respectively; percentage difference, Δ = +2.4%) and the final infiltration rate (ir = 18.9 and 16.4 mm/h; Δ = -13.5%). For the P2 plot (Fig. 3b), simulated rainfall rates were very similar in the two RSs at the beginning of the simulation but later, they diverged a little since rainfall intensities decreased during the run at a different rate (final rainfall rate 8.6% and 1.7% smaller than the initial one for the first and the second RS, respectively). An almost perfect overlap of the temporal behaviours of both *r* and *ir* can be observed until rainfall rates remained very similar. Moreover, the time at which $r = ir$ was reached did not differ between the two RSs (nearly 1 h). For both *r* and *ir*, the similarity of the temporal behaviours in the two RSs remained perceivable, but it was less evident during the later stage of the run. Finally, similarities were detected with reference to the final runoff rate (r = 50.2 and 53.8 mm/h for RS1 and RS2, respectively; Δ = +7.0%) and the final infiltration rate (ir = 11.8 and 12.6 mm/h; Δ = +6.4%). Therefore, the two subsequent simulations on each plot yielded overall a similar information on the dynamics of the runoff and infiltration process. This similarity was perceived for an area (internal ring) smaller than that of the plot both when a complete plot wetting preceded the partial wetting (P1) and when the partial wetting preceded the complete plot wetting (P2).

3.2. Soil changes during a period of intermittent rainstorms

The soil changes during intermittent rainfalls were explored by analyzing the results obtained in the type-B experiment, which included four RSs, performed approximately every 7 days starting from an initial condition of tilled soil (Table 1). With reference to the four rainfall simulations (denoted RS1, RS2, RS3 and RS4), the rainfall depth per simulation was equal on average to 148 mm (coefficient of variation, CV = 5.1%) for the P1 and to 130 mm (CV = 6.5%) for the P2.

As obvious, a RS determined a rapid increase of w and θ ($w_f > w_{in}$ and $\theta_f > \theta_i$) whereas redistribution and evaporation between two subsequent RSs reduced the soil water content (w_i and θ_i before a RS < w_f and θ_f at the end of the previous RS) (Fig. 4). However, these soil drying processes were not enough to attain stable w_i and θ_i values during the entire experimental period. In particular, w_i and θ_i were lowest for the first RS (w_i = 0.05–0.06 g/g and θ_i = 0.12–0.14 m^3/m^3, depending on the plot) and higher for the second (w_i = 0.11 g/g and θ_i = 0.20–0.21 m^3/m^3) and the subsequent RSs, for which they remained nearly stable or increased moderately ($w_i \leq$ 0.13 g/g and $\theta_i \leq$ 0.23–0.25 m^3/m^3) (Fig. 4 a,b). Therefore, the consequence of the alternation between a nearly sudden wetting event and a multi-day drying period was that a given amount of water (130–148 mm) falling on the initially dry soil (RS1) was enough to determine an appreciable increase in the subsequent w_i and θ_i values. However, the initial soil water content did not change appreciably between the last three RSs, notwithstanding that the same amount of rainfall was repeatedly applied at a fixed time interval. In other words, the effect of soil wetting prevailed over those of drying at the beginning of the experiment but later, wetting and drying effects became more balanced in this silty-clay soil.

The final gravimetric soil water content was highest after the first RS (w_f = 0.31–0.32 g/g, depending on the plot). Then, w_f decreased a little, and it stabilized at 0.28–0.29 g/g for the last two RSs. Even θ_f was highest at the end of the first RS (θ_f = 0.35–0.38 m^3/m^3, depending on the plot). However, θ_f was lowest after the second RS (θ_f = 0.29–0.30 m^3/m^3), and it increased up to 0.34 m^3/m^3 for the last two RSs. Therefore, the final soil water content reached a maximum when the porous medium was initially dry, and it was lower when the soil was initially wetter. This result was consistent with the Cislerova et al. (1988) conclusion that air entrapment in large pores sealed off by water films increases drastically at higher initial moisture contents. However, other explanations, such as a progressive decrease of total pore space during the subsequent RSs, also appeared plausible.

A small and non-monotonic increase of $\rho_{b,i}$ was detected in the passage from the first to the last RS (Fig. 4c and 4d). For six of the seven possible comparisons, the dry soil bulk density after rainfall was greater

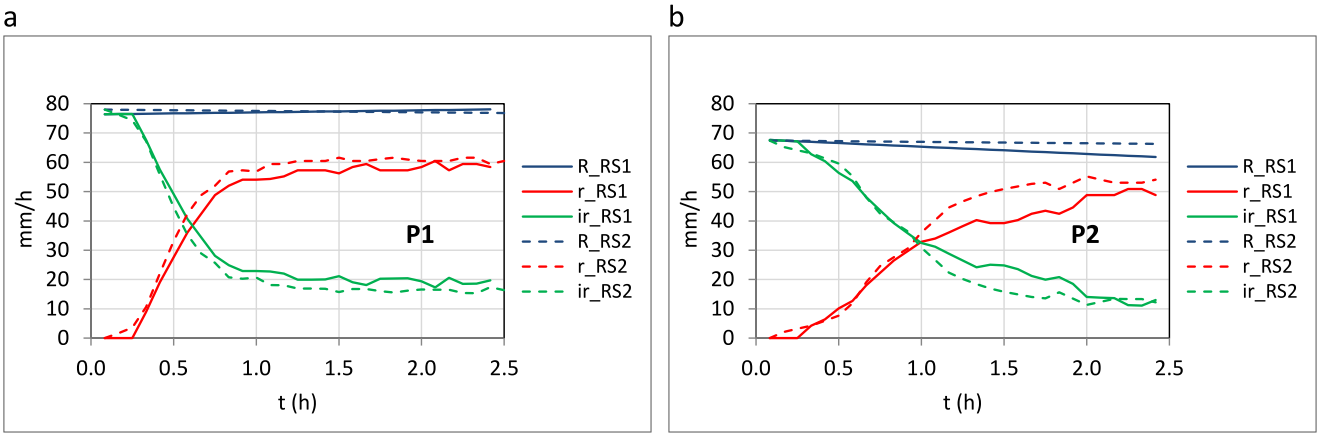

Fig. 3. Rainfall rate, *R*, runoff rate, *r*, and infiltration rate, *ir*, for the RS1 and RS2 of type-A experiment in the internal ring of P1 **(a)** and P2 **(b)** plots.

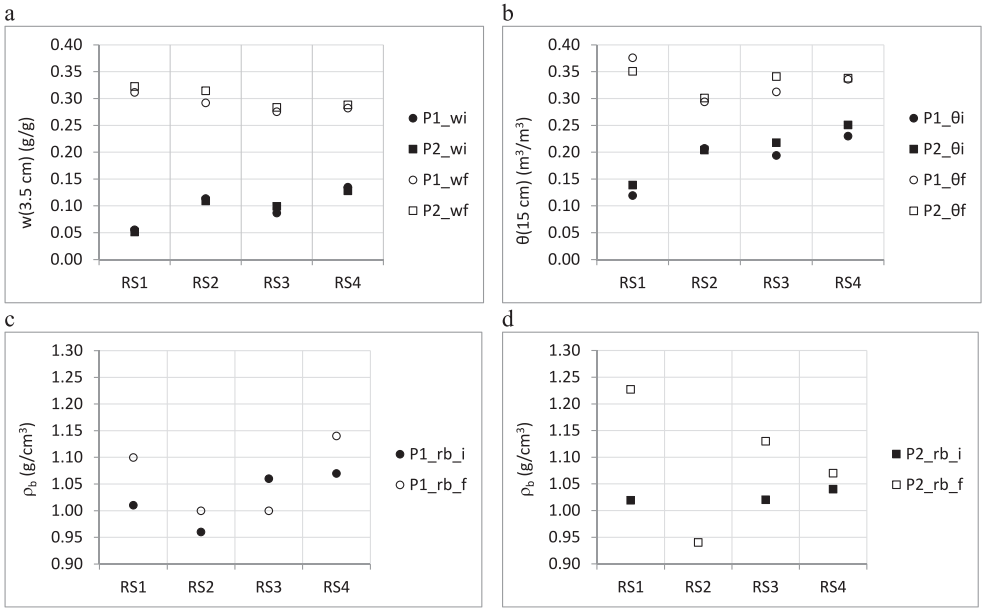

Fig. 4. **(a)** Gravimetric water content of the upper 3.5 cm of the soil before, w_i, and after, w_f, each rainfall simulation RS; **(b)** volumetric water content of the upper 15 cm of the soil before, θ_i, and after, θ_f, each simulated rainfall; dry soil bulk density before, $\rho_{b,i}$, and after, $\rho_{b,f}$, each RS for plots P1 **(c)** and P2 **(d)**. Type B experiment consisting of initial tillage followed by four RSs, lasting between 90 and 135 min, and spaced about seven days apart.

than the initial one. Therefore, there were signs of a more compacted soil surface at the beginning of a new RS during the experimental period, although these signs were overall weak. The indication of more compaction at the end of a RS was clearer. However, even this last result should be considered with some caution since it cannot be excluded that some extra compaction occurred when the very wet soil was sampled.

For both plots, there was a clear difference between the first RS and the other three RSs concerning both t_{ps} and t_{ds} (Fig. 5). In particular, with the first RS, free water appeared on the soil surface 31–36 min after rainfall started and other 25–30 min were necessary to collect runoff at the base of the plot. For the other RSs, t_{ps} did not exceed 7 min and the delay time, that is $t_{ds} - t_{ps}$, was 3 min at the most.

Both S and K_s decreased during the experimental period, and the two plots showed similarities regarding these two soil hydrodynamic properties (Fig. 6). The decrease from the first to the last RS was more appreciable for S (by 2.9–3.1 times, depending on the plot) than K_s (1.4–2.2 times). A rather abrupt decrease of S was recorded between the first two RSs, and subsequently, S continued to decrease at a lower rate. For K_s, the reduction from RS1 to RS4 was more gradual.

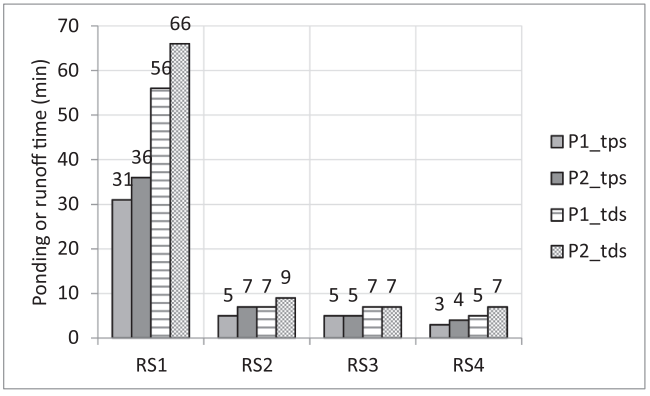

Fig. 5. Time to incipient ponding, t_{ps}, and time to runoff, t_{ds}, for each simulated rainfall in P1 and P2 plots. Type B experiment consisting of initial tillage followed by four RSs, lasting between 90 and 135 min, and spaced about seven days apart.

For both properties, the data obtained in the two plots described a single relationship with both θ_i and h_{cum} (Fig. 7) and both relationships for a given soil hydrodynamic parameter were statistically significant according to a two-tailed t-test at a probability level of 0.05. However, S was better correlated with θ_i than h_{cum} by a power relationship ($R^2 = 0.96$), while K_s was better correlated with h_{cum} than θ_i by a logarithmic relationship ($R^2 = 0.83$).

The comparison between the first and the last RS revealed that, at the end of the experimental period, λ_m increased by 2.3–3.8 times, depending on the plot, N_0 decreased by 59–297 times and the total area occupied by the λ_m pores per unit infiltration surface decreased by 11–21 times (Table 2). Therefore, an increase of the initial soil water content associated with a periodical mechanical disturbance of the infiltration surface due to rainfall impact made the effect of gravity as the infiltration driving force more relevant (Ndiaye et al., 2005), but it also induced a decrease of the fraction of the soil surface through which infiltration occurred (Souza et al., 2014).

3.3. Relationship between K_s and rainfall kinetic energy

The K_s value for each RS (Table 1) was computed by eq.(1) and the complete dataset was analysed to evaluate the K_s behaviour during repeated rainfalls, starting from initial tillage. The specific aim was to verify if the cumulative rainfall energy explained changes in K_s during a period of intermittent rainfalls.

To describe the functional relationship between K_s and the cumulative rainfall energy, E (kJ /m^2), since tillage (including the energy of IW when applied), the dataset composed of $N = 28$ (K_s, E) data pairs ($N = 14$ for the P1 and $N = 14$ for P2 derived from the entire plots in the experiments type B and C and from the internal plots in experiment type A), was used in a regression analysis. Based on the coefficient of determination, R^2, the best interpolating function ($R^2 = 0.17$) was of a power type (Fig. 8). The model was statistically significant, although it had a high percentage of unexplained variance due to a relevant data scattering that also characterised the single plots data. Moreover, the use of different models for the two plots was not justified from a statistical point of view since the residual variance increase of the single model was not statistically significant (significance level, $\alpha = 0.01$) compared to the models developed on the data of each plot. Therefore, the power

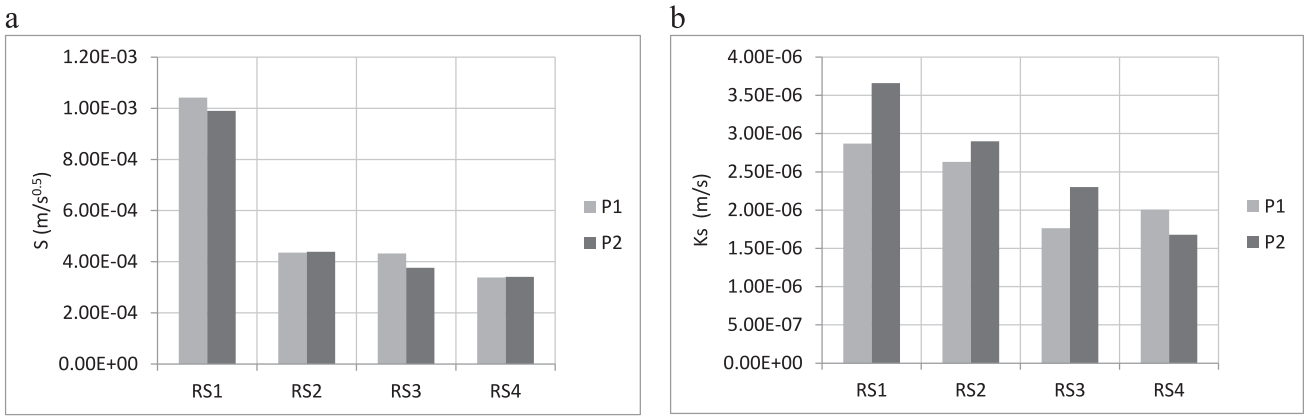

Fig. 6. Soil sorptivity, S, **(a)** and saturated soil hydraulic conductivity, K_s, **(b)** for each simulated rainfall in P1 and P2 plots. Type B experiment consisting of initial tillage followed by four RSs, lasting between 90 and 135 min, and spaced about seven days apart.

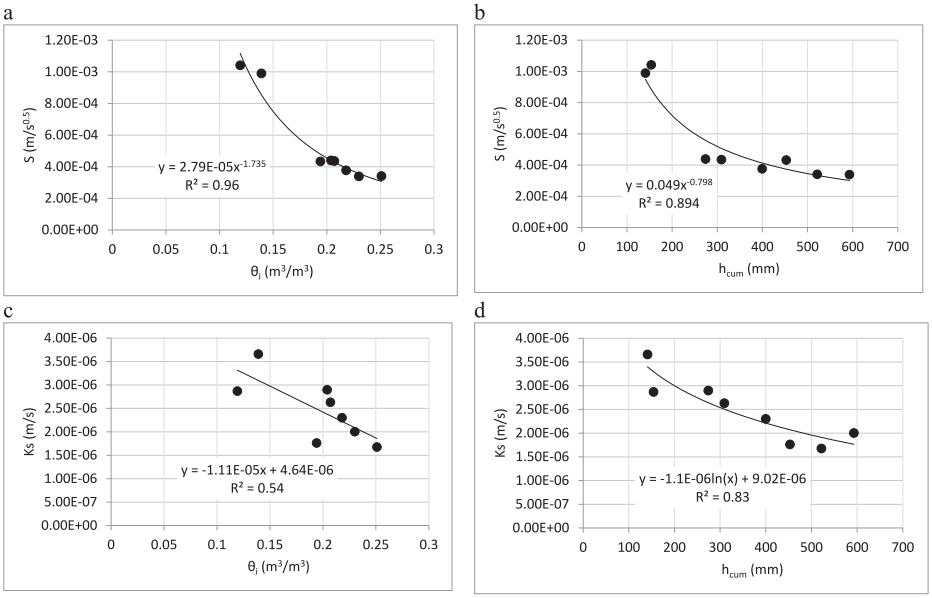

Fig. 7. Soil sorptivity, S, against antecedent soil water content, θ_i **(a)**; S against cumulated rainfall depth by the end of the considered rainfall simulation, h_{cum} **(b)**; Saturated soil hydraulic conductivity, K_s, against θ_i **(c)**; K_s, against h_{cum} **(d).** Data of both P1 and P2 plots related to the type B experiment consisting of initial tillage followed by four RSs, lasting between 90 and 135 min, and spaced about seven days apart.

Table 2
Flow-weighted mean pore radius at the antecedent potential, λ_m, concentration of λ_m pores, N_0, and total area occupied by the λ_m pores per unit infiltration surface at the beginning and the end of the experimental period in the two sampled plots. Type B experiment consisting of initial tillage followed by four RSs, lasting between 90 and 135 min, and spaced about seven days apart.

Plot	Period	λ_m (m)	N_0 (number of pores/m^2)	Total area occupied by the λ_m pores (m^2/m^2)
1	Initial	9.16×10^{-6}	9.50×10^{7}	0.0250
	Final	3.47×10^{-5}	3.20×10^{5}	0.0012
2	Initial	1.37×10^{-5}	2.42×10^{7}	0.0143
	Final	3.12×10^{-5}	4.09×10^{5}	0.0013

relationship of Fig. 8 can be considered valid for the experimental site.

Fig. 8 also shows an envelope curve, representing the maximum K_s value expected for a fixed rainfall energy accumulated starting from the last tillage. Although K_s scattering under the curve was noticeable, the envelope curve suggested that a distinction can be made between possible and unexpected values of K_s. In particular, the expected range of possible K_s values became smaller and it tended to settle on smaller values as E increased. For example, the expectation was to obtain $K_s \leq 30$ mm/h for $E = 2$ kJ/m^2 and $K_s \leq 5$ mm/h for $E = 8$ kJ/m^2.

Fig. 9 shows the means of K_s plotted against the means of E for each RS. From six to eight data points were averaged for the first three RSs, while only two data points were available regarding the fourth RS. Concerning the first three RSs, the $K_s(E)$ data described a decreasing relationship having an exponential shape. A relationship fitted on three data points could be considered intrinsically weak, notwithstanding that it was statistically significant at the 0.05 probability level. However, its reliability was supported by the circumstances that i) each individual data point plausibly had satisfactory representativeness since at least six individual data were averaged, and ii) several other investigations have reported an exponential relationship between K_s and E (e.g., Brakensiek and Rawls, 1983; Chu et al., 1986; Mügler et al., 2019). According to the fitted relationship, K_s was predicted to decrease by more than eight times as E increases from 0 to 5 kJ/m^2 (from 36.8 to 4.5 mm/h). Extrapolating the fitted $K_s(E)$ relationship to the highest experimental mean value of E (8.1 kJ/m^2) yielded a predicted K_s value (1.3 mm/h) that was nearly 29 times smaller than that corresponding to $E = 0$,

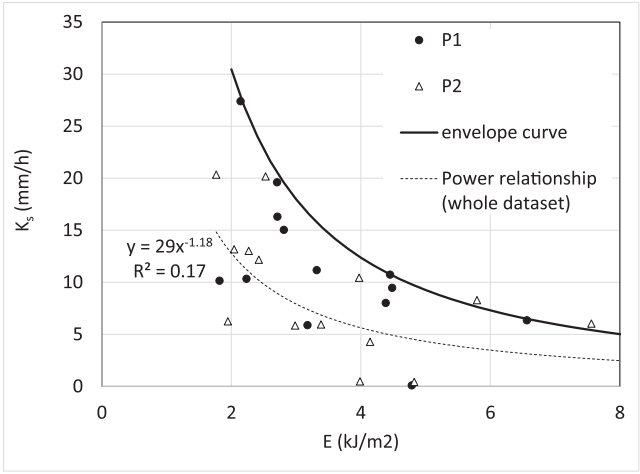

Fig. 8. Scatter plot of the saturated hydraulic conductivity, K_s, values against the cumulated rainfall energy, E, for the type-A, type-B and type-C experiments in P1 and P2 plots.

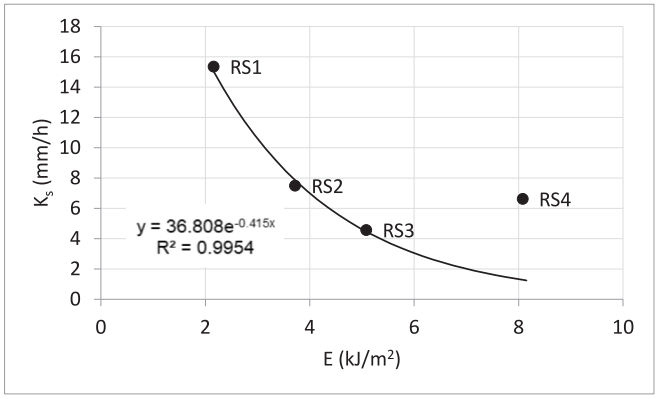

Fig. 9. Scatter plot of the saturated hydraulic conductivity, K_s, against the cumulated rainfall energy, E, (data from all the experiments averaged by rainfall simulation number after soil tillage).

suggesting a noticeable variation of K_s with E. However, the predicted K_s value for $E = 8.1$ kJ/m^2 was almost five times lower than the experimental K_s value (6.6 mm/h).

4. Discussion

Most of the available information on the effects of lateral divergence of infiltrated water refers to a process through a horizontal soil surface (e.g., Reynolds and Elrick, 1990, 2002; Reynolds et al., 2002). In this case, the lateral divergence has a less relevant effect on steady-state infiltration rate as the size of the source increases (Reynolds et al., 2002), and the importance of the initial absorption period decreases as the antecedent soil water content increases (Youngs et al., 1995). Moreover, although slope effects on infiltration have been studied also recently (Chen and Young, 2006; Morbidelli et al., 2015; Morbidelli et al., 2016), little is known on the effect of slope on a rainfall infiltration process occurring through a more or less small area. Therefore, the type-A experiment carried out in this investigation explores a rather novel scenario for which there is not much information in the literature. The disadvantage of this novelty is that the results cannot easily be discussed in light of a well-established theoretical treatment of the problem.

It could be presumed that, in the P1 plot (Fig. 3a), a similarity between the two RSs was detected because the complete plot wetting on the first date maintained the initial water content of the sub-surface layer relatively high even during the second event, and this circumstance mitigated lateral divergence of the infiltrated water. In other words, lateral divergence was small for RS1 because the area surrounding the ring was also wetted. Concerning RS2, lateral divergence remained small because the sub-surface soil was initially wet. This interpretation could suggest that lateral divergence at the sampled site did not appreciably influence the infiltration process when the initial soil water content was relatively high. However, the experiment on the P2 plot (Fig. 3b) suggested that lateral divergence was not relevant in general. In this plot, lateral divergence phenomena were expected to occur at the highest rate for RS1 since only the soil confined by the ring was wetted. Lateral divergence was expected to be lower and nearly negligible for RS2 since all the plot area was wetted in this case. Taking into account that divergence was minimized for RS1 in the P1 plot and RS2 in the P2 plot and that the measured runoff and infiltration processes did not differ appreciably from those detected in a more favourable condition for occurrence of lateral divergence phenomena (RS2 in the P1 plot and RS1 in the P2 plot), this investigation induced to believe that lateral divergence did not influence appreciably the runoff-infiltration dynamics in the sampled plots. Therefore, the assumption that the established process in a plot was essentially unaffected by lateral divergence phenomena appeared plausible.

This investigation revealed a delay between runoff and ponding times (Fig. 5), which was not surprising, being documented even at very small spatial scales (Di Prima et al., 2017). A decrease of t_{ps} during the experimental period is consistent with the increase of θ_i (Fig. 4b) since the time to ponding decreases as the antecedent soil wetness increases (Assouline, 2013). However, Morin and Benyamini (1977) suggested that the soil moisture regime could not directly affect infiltration when a crust is formed by raindrop impact; indeed, this crust has a much lower conductivity than the soil had before the crust formation. In this case, the crust becomes the governing factor of the infiltration process. A physical alteration of the soil surface exposed to rainfall appeared plausible because t_{ds} decreased appreciably from the first to the subsequent RSs, suggesting that raindrop impact had a levelling effect that made runoff transport easier (Fohrer et al., 1999; Ndiaye et al., 2005). Consequently, surface roughness formed by tillage was likely effective in retarding flow transport only for a short time since the surface became smoother after the first rainfall event (Vinci et al, 2020).

Attempting to explore changes in soil hydrodynamic parameters (Fig. 7), using θ_i as the independent variable means assuming that the main factor controlling these parameters was the soil wetness condition before the rainfall event. Taking into account that cumulative rainfall since tillage can be viewed as an index of the dissipated energy (Freebairn et al., 1989; Ndiaye et al., 2005), using h_{cum} as the independent variable means assuming that the cumulated energy dissipated at the soil surface since tillage influenced S and K_s. Although the link between θ_i and h_{cum} is known, these two quantities are not interchangeable with each other. For example, the mean θ_i value did not change between RS2 and RS3 (0.21 m^3/m^3, Fig. 4b), although h_{cum} was equal to 292 mm for RS2 and 426 mm for RS3.

The inverse relationship between S and θ_i (Fig. 7a) was physically sound, qualitatively supporting the presumption that the sampled soil was ideal. The fact that t_{ps} decreased in initially wetter soil conditions reinforced this interpretation. However, K_s was not stable, denoting that the soil experienced some structural modification during the experimental period. In other words, the K_s data provided clearer information on soil structure dynamics than the S data since, in an ideal porous medium, S depends on the antecedent soil water content but K_s should not vary. The changes in K_s were not substantial considering that, according to Elrick and Reynolds (1992), differences in K_s by a factor of two or three could be considered negligible, at least for some practical purposes. Soil wetting modifies structure through a variety of mechanisms such as slaking, swelling, dispersion and raindrop impact (Le Bissonnais, 1996; Tanner et al., 2021). An inverse relationship between K_s and θ_i (Fig. 7c) can suggest that K_s decreased during the experimental

period as a consequence of soil swelling, reducing macroporosity, and maybe some weakening of the interparticle bonds in wetter soil conditions, making particle dispersion and subsequent pore-clogging easier (Chaudhari, 2001; Lado et al., 2004; Todisco et al., 2022). Perhaps, some slaking of the initially dry soil aggregates also occurred at the beginning of the experiment (Le Bissonnais, 1996), and the formed micro-aggregates were mobile throughout the profile, even during the subsequent RSs. However, K_s was better correlated with h_{cum} than θ_i, (Fig. 7) and the former variable is more expressive of the mechanical breakdown effects occurring at the soil surface as a consequence of raindrops impact as compared with the latter one. This circumstance, in conjunction with the decrease of the delay time, $t_{ds} - t_{ps}$, soon after the first RS, suggested that rainfall altered the soil surface, smoothing out the original micro-topography by infilling up the depressions by sediments detached from the crests (Ndiaye et al., 2005). Probably, soil structural breakdown by rain impact and surface capping or sealing also occurred (Messing and Jarvis, 1993) in accordance with other rainfall simulation experiments (Ndiaye et al., 2005).

Both S and K_s appeared less temporally variable in the latter part of the experimental period than in the earlier stage (Fig. 7). Therefore, a soil hydraulic characterization performed soon after tillage has a limited temporal validity since the measured soil properties probably will change rapidly. Instead, characterizing a tilled soil after a sequence of wetting and drying events seems more appropriate in a hydrological perspective, that is to describe the soil's response during some hydrologically relevant phenomena such as formation of hortonian runoff (Auteri et al., 2020).

Saturated soil hydraulic conductivity can be expected to decrease during a continuous rainfall event (Mügler et al., 2019) since, as the exposure to rainfall continues, further compaction by raindrops and swelling and collapse in the wetted deeper aggregates can occur (Assouline, 2004). According to this investigation, rainfall intermittency did not impede the detection of an inverse relationship between K_s and E (Fig. 8), suggesting that the mentioned soil alteration phenomena had a relevant effect on K_s even if rainfall was not continuous. However, it is known that the duration of the drying period after a rainfall event can influence the subsequent infiltration process (Morin and Benyamini, 1977). Therefore, a point that should be investigated in more detail is establishing if at least a part of the unexplained variance in the fitted $K_s(E)$ relationship (Fig. 8) could depend on drying and soil reorganization processes that perhaps occurred in the time intervals between two subsequent rainfall events (Todisco et al., 2022). In other terms, it should be verified if the $K_s(E)$ relationship changes in shape and fitting quality as the duration of the drying period varies. This check has practical interest since the intermittence of natural rainfall events is unpredictable.

The inverse relationship between K_s and E (Figs. 8 and 9) reinforced the validity of previous suggestions on the need to assure the hydrological relevance of the experimentally determined surface soil hydrodynamic properties. In other terms, the experiment yielding surface soil hydrodynamic parameters has to be adapted so that the hydrological process of interest can properly be interpreted and simulated (Auteri et al., 2020). In many instances, emphasis is put on the fact that obtaining reliable soil hydrodynamic data in the field requires avoiding or at least reducing as much as possible any soil alteration during the experiment (Reynolds, 2008; Angulo-Jaramillo et al., 2016; Khodaverdiloo et al., 2017; Lassabatere et al., 2019). According to this investigation, this suggestion should not be considered valid in general since soil alteration appears almost unavoidable during a hydrological event. Instead, given the dynamic nature of the porous medium, the experimental methodology for determining K_s should be consistent with the hydrological question that one intends to address (Auteri et al., 2020). Otherwise, the risk could be obtaining excessively high K_s values (Ben-Hur et al., 1987; Cerdà, 1999; van de Giesen et al., 2000) that do not describe the soil appropriately.

The most obvious interpretation of the discrepancy between the experimental and the predicted K_s value for the fourth RS (Fig. 9) was that the mean K_s value for this RS was not reliable since only two individual data points were averaged in this case. Therefore, it appears plausible that, with more data for the fourth RS, the experimental mean of K_s could be closer to the predicted one, denoting that the fitted $K_s(E)$ relationship can be extrapolated in the range of higher E values. The physical reason why this result could be obtained is that the development of a seal layer can be considered a continuous process that ends when there is no more space for compaction and other soil alteration processes (Assouline, 2004). In this case, K_s should stabilize at the lowest possible value. However, another interpretation can also be proposed assuming that even the last K_s data point of Fig. 9 was reasonably reliable. In particular, it could be suggested that three subsequent rainfall events were enough to produce all possible soil alteration. During the fourth event, the raindrop impact disturbed the sealed layer that was partially disrupted. Hence infiltration rates and K_s increased. As compared with the development stage, there is less literature documenting rainfall-induced increase of K_s as a consequence of the raindrops impact on an already altered soil layer (Neave and Rayburg, 2007). Therefore, more data should be collected in the perspective to more confidently capture the soil behaviour in an advanced stage of seal layer formation.

5. Conclusions

A methodology for determining the hydrodynamic characteristics of the soil developed with reference to an infiltration process not influenced by the lateral divergence of the wetting front also appears to be usable in an experimental installation in which the divergence mentioned above cannot be excluded. This conclusion, although based on a small number of experiments, is encouraging and deserves further confirmation since the methodology to derive soil hydrodynamic parameters is easy to use, making use of quantities that are routinely measured in rainfall-runoff experiments with a rain simulator.

During a succession of rainfalls on an initially dry silty-clay-loam soil with wetting and drying cycles with intervals of about 7 days, there is a decrease of both S and K_s, but in different ways, that is abrupt for S and more gradual for K_s. Therefore, the temporal dynamics of the hydrodynamic properties of the soil vary with the property considered. A hydraulic characterization carried out with reference to K_s allows for detecting physical impacts of rainfall that are not perceptible, or are less clearly detectable, when S is determined, given the latter parameter also depends on the initial water content of the soil.

For predicting and simulating the rainfall-runoff transformation process, it is advisable not to limit the investigation to a hydraulic characterization carried out immediately or shortly after tillage. In fact, it is expected that drying-wetting cycles following tillage can significantly modify the soil hydrodynamic properties.

The analysis confirmed that K_s decreases as the overall energy dissipated at the soil surface increases. In particular, the range of possible K_s values decreases with more dissipated rainfall energy at the soil surface. A consequence of this finding is that less K_s data could be enough to characterize the soil after several wetting and drying cycle than shortly after tillage. However, the investigation also induced not to exclude that, for very high energy values, a recovery mechanism of the hydraulic properties of the altered/compacted layer can occur, for example, with a detachment of surface particles which causes the re-exposure of previously occluded surface macropores. The recovery of the hydraulic properties of the soil is not widely documented in the scientific literature. Therefore, it is advisable first to check whether the result obtained is incidental and perhaps linked to the available experimental information. Should it be confirmed, the next step will be to establish the causes unequivocally. Testing the effects of plot length on the determination of soil hydrodynamic parameters in a practical range, that is, no more than a few meters, could also be advisable to delineate better the link between the experimental installation and the

hydrological usefulness of the collected data.

This investigation has laid a sound methodological basis for a hydrologically relevant soil hydraulic characterization. Once the experimental installation has been realized, it becomes relatively easy to quantitatively assess the soil behaviour under rainfall scenarios differing, for example, by the shower duration or the interval between showers.

Declaration of Competing Interest

The authors declare that they have no known competing financial interests or personal relationships that could have appeared to influence the work reported in this paper.

Data availability

Data will be made available on request.

References

Angulo-Jaramillo, R., Bagarello, V., Iovino, M., Lassabatere, L., 2016. Infiltration Measurements for Soil Hydraulic Characterization. Springer International Publishing, AG Switzerland, p. 386.

Assouline, S., 2004. A Critical Review of Observations, Conceptual Models, and Solutions. Vadose Zone J. 3 (2), 570–591.

Assouline, S., 2013. Infiltration into soils: conceptual approaches and solutions. Water Resour. Res. 49 (4), 1755–1772.

Assouline, S., Mualem, Y., 1997. Modeling the dynamics of seal formation and its effect on infiltration as related to soil and rainfall characteristics. Water Resour. Res. 33 (7), 1527–1536.

Assouline, S., Mualem, Y., 2006. Runoff from heterogeneous small bare catchments during soil surface sealing. Water Resour. Res. 42, W12405.

Auteri, N., Bagarello, V., Concialdi, P., Iovino, M., 2020. Testing an adapted beerkan infiltration run for a hydrologically relevant soil hydraulic characterization. J. Hydrol. 584, 12469714.

Bagarello, V., Baiamonte, G., Caia, C., 2019. Variability of near-surface saturated hydraulic conductivity for the clay soils of a small Sicilian basin. Geoderma. 340, 133–145.

Ben-Hur, M., Agassi, M., 1997. Predicting interrill erodibility factor from measured infiltration rate. Water Resour. Res. 33 (10), 2409–2415.

Ben-Hur, M., Shainberg, I., Morin, J., 1987. Variability of infiltration in a field with surface-sealed soil. Soil Sci. Soc. Am. J. 51, 1299–1302.

Bhattacharyya, R., Prakash, V., Kundu, S., Gupta, H.S., 2006. Effect of tillage and crop rotations on pore size distribution and soil hydraulic conductivity in sandy clay loam soil of the Indian Himalayas. Soil Till. Res. 86, 129–140.

Bielders, C., Baveye, P., 1995. Processes of structural crust formation on coarse-textured soils. Eur. J. Soil Sci. 46, 221–232.

Bielders, C.L., Baveye, P., Wilding, L.P., Drees, L.R., Valentin, C., 1996. Tillage induced spatial distribution of surface crusts on a sandy paleustult from Togo. Soil Sci. Soc. Am. J. 60, 843–855.

Brakensiek, D.L., Rawls, W.J., 1983. Agricultural management effects on soil water processes. Part II. Green and Ampt parameters for crusting soils. T. ASAE. 26 (6), 1753–1757.

Carter, M.R., Kunelius, H.T., 1986. Comparison of tillage and direct drilling for Italian ryegrass on the properties of a fine sandy loam soil. Can. J. Soil Sci. 66, 197–207.

Cerdà, A., 1999. Seasonal and spatial variations in infiltration rates in badland surfaces under Mediterranean climatic conditions. Water Resour. Res. 35 (1), 319–328.

Chahinian, N., Moussa, R., Andrieux, P., Voltz, M., 2006. Accounting for temporal variation in soil hydrological properties when simulating surface runoff on tilled plots. J. Hydrol. 326, 135–152.

Chaudhari, S.K., 2001. Saturated hydraulic conductivity, dispersion, swelling and exchangeable sodium percentage of different textured soils as influenced by water quality. Commun. Soil Sci. Plant Anal. 32, 2439–2455.

Chen, L., Young, M.H., 2006. Green-Ampt infiltration model for sloping surfaces. Water Resour. Res. 42, W07420.

Chu, S.T., 1985. Modeling infiltration into tilled soil during non-uniform rainfall. T. ASAE. 28 (4), 1226–1232.

Chu, S.T., Onstad, C.A., Rawls, W.J., 1986. Field Evaluation of Layered Green-Ampt Model for Transient Crust Conditions. T. ASAE. 29 (5), 1268–1272.

Cislerova, M., Simunek, J., Vogel, T., 1988. Changes of steady-state infiltration rates in recurrent ponding infiltration experiments. J. Hydrol. 104, 1–16.

Coutadeur, C., Coquet, Y., Roger-Estrade, J., 2002. Variation of hydraulic conductivity in a tilled soil. Eur. J. Soil Sci. 53, 619–628.

Di Prima, S., Bagarello, V., Lassabatere, L., et al., 2017. Comparing Beerkan infiltration tests with rainfall simulation experiments for hydraulic characterization of a sandy-loam soil. Hydrol. Process. 31, 3520–3532.

Elrick, D.E., Reynolds, W.D., 1992. Methods for analyzing constant-head well permeameter data. Soil Sci. Soc. Am. J. 56 (1), 320–323.

Farres, P., 1978. Role of time and aggregate size in the crusting process. Earth Surf Processes 3 (3), 243–254.

Fohrer, N., Berkenhagen, J., Hecker, J.-M., Rudolph, A., 1999. Changing soil and surface conditions during rainfall. Single rainstorm/subsequent rainstorms. Catena. 37 (3–4), 355–375.

Freebairn, D.M., Gupta, S.C., Onstad, C.A., Rawls, W.J., 1989. Antecedent rainfall and tillage effects upon infiltration. Soil Sci. Soc. Am. J. 53, 1183–1189.

Haruna, S.I., Anderson, S.H., Nkongolo, N.V., Zaibon, S., 2018. Soil hydraulic properties: Influence of tillage and cover crops. Pedosphere. 28 (3), 430–442.

Haverkamp, R., Ross, P.J., Smettem, K.R.J., Parlange, J.Y., 1994. Three dimensional analysis of infiltration from the disc infiltrometer. Part 2. Physically based infiltration equation Water Resour. Res. 30 (11), 2931–2935.

Heard, J.R., Kladivko, E.J., Mannering, J.V., 1988. Soil macroporosity, hydraulic conductivity and air permeability of silty soils under long-term conservation tillage in Indiana. Soil Till. Res. 11, 1–18.

Horton, R.E., 1939. Analysis of runoff-plat experiments with varying infiltration-capacity. Eos Trans. AGU. 20 (4), 693–711.

Iovino, M., Castellini, M., Bagarello, V., Giordano, G., 2016. Using Static and Dynamic Indicators to Evaluate Soil Physical Quality in a Sicilian Area. Land Degrad. Develop. 27, 200–210.

Joschko, M., Sochtig, W., Larink, O., 1992. Functional relationship between earthworm burrows and soil water movement in column experiments. Soil Biol. Biochem. 24, 1545–1547.

Kargas, G., Kerkides, P., Sotirakoglou, K., Poulovassilis, A., 2016. Temporal variability of surface soil hydraulic properties under various tillage systems. Soil Till. Res. 158, 22–31.

Kheyrabi, D., Monnier, G., 1968. Etude expérimentale de l'influence de la composition granulométrique des terres sur leur stabilité structurale. Ann. Agron. 19, 129–152.

Khodaverdiloo, H., Cheraghabdal, H.K., Bagarello, V., Iovino, M., Asgarzadeh, H., Dashtaki, S.G., 2017. Ring diameter effects on determination of field-saturated hydraulic conductivity of different loam soils. Geoderma 303, 60–69.

Lado, M., Ben-Hur, M., Shainberg, I., 2004. Soil Wetting and Texture Effects on Aggregate Stability, Seal Formation, and Erosion. Soil Sci. Soc. Am. J. 68, 1992–1999.

Lassabatere, L., Di Prima, S., Bouarafa, S., Iovino, M., Bagarello, V., Angulo-Jaramillo, R., 2019. BEST-2K method for characterizing dual-permeability unsaturated soils with ponded and tension infiltrometers. Vadose Zone J. 18 (1), 1–20.

Le Bissonnais, Y., 1989. Contribution àl'étude de la dégradation structurale superficielle: analyse des processus de microfissuration des agrégats par l'eau. Science du Sol 27, 187–199.

Le Bissonnais, Y., 1996. Aggregate stability and assessment of soil crustability and erodibility: I. Theory and methodology. Eur. J. Soil Sci. 47, 425–437.

Messing, I., Jarvis, N.J., 1993. Temporal variation in the hydraulic conductivity of a tilled clay soil as measured by tension infiltrometers. J. Soil Sci. 44, 11–24.

Morbidelli, R., Saltalippi, C., Flammini, A., Cifrodelli, M., Corradini, C., Govindaraju, R. S., 2015. Infiltration on sloping surfaces: Laboratory experimental evidence and implications for infiltration modelling. J. Hydrol. 523, 79–178.

Morbidelli, R., Saltalippi, C., Flammini, A., Cifrodelli, M., Picciafuoco, T., Corradini, C., Govindaraju, R.S., 2016. Laboratory investigation on the role of slope on infiltration over grassy soils. J. Hydrol. 543, 542–547.

Morin, J., Benyamini, Y., 1977. Rainfall infiltration into bare soils. Water Reosur. Res. 13 (5), 813–817.

Mualem, Y., Assouline, S., Rohdenburg, H., 1990. Rainfall induced soil seal (A) A critical review of observations and models. Catena. 17 (2), 185–203.

Mügler, C., Ribolzi, O., Janeau, J.-L., Rochelle-Newall, E., Latsachack, K., Thammahacksa, C., Viguier, M., Jardé, E., Henri-Des-Tureaux, T., Sengtaheuanghoung, O., Valentin, C., 2019. Experimental and modelling evidence of short-term effect of raindrop impact on hydraulic conductivity and overland flow intensity. J. Hydrol. 570, 401–410.

Ndiaye, B., Esteves, M., Vandervaere, J.P., Lapetite, J.M., Vauclin, M., 2005. Effect of rainfall and tillage direction on the evolution of surface crusts, soil hydraulic properties and runoff generation for a sandy loam soil. J. Hydrol. 307, 294–311.

Neave, M., Rayburg, S.C., 2007. A field investigation into the effects of progressive rainfall-induced soil seal and crust development on runoff and erosion rates: The impact of surface cover. Geomorphology. 87 (4), 378–390.

Panini, T., Torri, D., Pellegrini, S., Pagliai, M., Sanchis, M.P.S., 1997. A theoretical approach to soil porosity and sealing development using simulated rainstorms. Catena. 31 (3), 199–218.

Reynolds, W.D., 2008. Saturated hydraulic properties: ring infiltrometer. In: Carter, M. R., Gregorich, E.G. (Eds.), Soil Sampling and Methods of Analysis, second ed. Can. Soc, Soil Sci, Boca Raton, FL, USA, pp. 1043–1056.

Reynolds, W.D., Elrick, D.E, 2002. Pressure infiltrometer In: J.H. Dane and G.C. Topp, editors, Methods of soil analysis. Part 4. Physical methods. SSSA Book Ser. 5. SSSA, Madison, WI. 826–836.

Reynolds, W.D., Elrick, D.E., 1990. Ponded infiltration from a single ring: I. Analysis of steady flow. Soil Sci. Soc. Am. J. 54, 1233–1241.

Reynolds, W.D., Gregorich, E.G., Curnoe, W.E., 1995. Characterisation of water transmission properties in tilled and untilled soils using tension infiltrometers. Soil Till. Res. 33, 117–131.

Reynolds, W.D., Elrick, D.E., Youngs, E.G., 2002. A single-ring and double- or concentric-ring infiltrometers. In: Dane, J.H., Topp, G.C. (Eds.), Methods of soil analysis. Part 4. Physical methods. Soil Science Society of America, Madison, Wisconsin, USA, pp. 821–826.

Roth, C.H., 1997. Bulk density of surface crusts: depth functions and relationships to texture. Catena. 29, 223–237.

Rousseva, S., Torri, D., Pagliai, M., 2002. Effect of rain on the macroporosity at the soil surface. European J. Soil Sci. 53 (1), 83–94.

Schröder, R., Auerswald, K., 2000. Modellierung des Jahresgangs der verschlämmungsinduzierten Abflussbildung in kleinen landwirtschaftlich genutzten Einzugsgebieten. Z. Kulturtechnik Landentwicklung 41, 167–172.
Souza, E.S., Antonino, A.C.D., Heck, R.J., Montenegro, S.M.G.L., Lima, J.R.S., et al., 2014. Effect of crusting on the physical and hydraulic properties of a soil cropped with Castor beans (Ricinus communis L.) in the northeastern region of Brazil. Soil Till. Res. 141, 55–61.
Tanner, S., Katra, I., Argaman, E., Ben-Hur, M., 2021. Mechanisms and processes affecting aggregate stability and saturated hydraulic conductivity of top and sublayers in semi-arid soils. Geoderma. 404, 115304.
Todisco, F., Vergni, L., Ceppitelli, R., 2023. Modelling the dynamics of seal formation and pore clogging in the soil and its effect on infiltration using membrane fouling models. J. Hydrol. 618, 129208.
Todisco, F., Vergni, L., Vinci, A., Torri, D., 2022. Infiltration and bulk density dynamics with simulated rainfall sequences. Catena. 218, 106542.
Touma, J., Voltz, M., Albergel, J., 2007. Determining soil saturated hydraulic conductivity and sorptivity from single ring infiltration tests. Eur. J. Soil Sci. 58, 229–238.
van De Giesen, N.C., Stomph, T.J., de Ridder, N., 2000. Scale effects of Hortonian overland flow and rainfall–runoff dynamics in a WestAfrican catena landscape. Hydrol. Process. 14, 165–175.
Vergni, L., Todisco, F., Vinci, A., 2018. Setup and calibration of the rainfall simulator of the Masse experimental station for soil erosion studies. Catena. 167, 448–455.
Vinci, A., Todisco, F., Vergni, L., Torri, D., 2020. A comparative evaluation of random roughness indices by rainfall simulator and photogrammetry. Catena. 188, 104468.
White, I., Sully, M.J., Melville, M.D., 1989. Use and hydrological robustness of time-to-incipient-ponding. Soil Sci. Soc. Am. J. 53 (5), 1343–1346.
Yoder, R.E., 1936. A direct method of aggregate analysis of soils and a study of the physical nature of erosion losses. J. Am. Soc. Agron. 28, 337–351.
Youngs, E.G., Leeds-Harrison, P.B., Elrick, D.E., 1995. The hydraulic conductivity of low permeability wet soils used as landfill lining and capping material: Analysis of pressure infiltrometer measurements. Soil Technol. 8 (2), 153–160.
Zobeck, T.M., Onstad, C.A., 1987. Tillage and rainfall effects on random roughness: A review. Soil Till. Res. 9 (1), 1–20.